



EUROPEAN ORGANIZATION FOR NUCLEAR RESEARCH

CERN-EP/80-154  
15 August 1980

DRIFT-TUBE ARRAYS FOR HIGH SPATIAL RESOLUTION

U. Becker

CERN, Geneva, Switzerland

M. Steuer

LAPP, Annecy, France

J. Burger and M. White

MIT, Cambridge, MA, USA

ABSTRACT

An array of 32 thin-walled drift tubes was traversed by a 20 GeV proton beam and the resulting track reconstructed. The spatial resolution was measured as a function of the number of individual coordinates recorded. The frequency of  $\delta$ -rays and the criteria for the rejection of non-statistically distributed coordinates were studied. A value of  $\sigma = (156 \pm 5) \mu\text{m}/\sqrt{N}$  was obtained using  $N$  drift tubes, while the accuracy of an individual tube was found to be  $\sigma_{\text{tube}} \approx 135 \mu\text{m}$ .

(Submitted to Nuclear Instruments and Methods)

## 1. INTRODUCTION

Charged-particle detectors for future storage-ring experiments<sup>1)</sup> will require high spatial resolution<sup>2)</sup> and compact design, combined with maximum operating reliability under high rate conditions. Thin-walled drift tubes meet the above requirements.

The arrays consisted of 32 drift tubes of 1 cm diameter with 0.25 mm aluminium walls. They had a length of 30 cm and a tungsten wire of 40  $\mu\text{m}$  in their centre. They were tested with 20 GeV protons at the CERN PS, with different gas mixtures and at beam rates up to 600 counts/s $\cdot$ cm. A spatial resolution of  $\sigma_{\text{tube}} \lesssim 135 \mu\text{m}$  has been achieved. Combining several tubes results in a substantial improvement in resolution. Measurements incompatible with probability criteria demanding a straight track are rejected and therefore most of the  $\delta$ -rays are eliminated.

These tubes are operating at present with excellent reliability under severe synchrotron radiation background at MARK J at PETRA<sup>3)</sup>.

## 2. SET-UP AND RESULTS

The beam  $b_{16}$  of the CERN PS was used for the studies. Figure 1 shows the test set-up. Protons of 20 GeV energy traverse an array of 32 drift tubes in a 2 mm wide beam, defined by the two counters trig 2 \* trig 3. Trig 1 is used for suppression of accidentals. The drift-tube array can be displaced perpendicular to the beam and sense-wire direction with an accuracy of 0.01 mm. The signal from the positive sense wire (typically at +2.20 kV) is shaped in a preamplifier and recorded in a LeCroy 2228 8-channel time-to-digital converter (TDC) with a resolution of 0.2 ns/channel. The start comes from the beam coincidence trig 1 \* \* trig 2 \* trig 3.

Two gas mixtures were measured: A - argon (55%)-ethane (45%) and B - argon (66%)-ethane (34%). For both mixtures the drift velocity across the tube radius was measured in 0.5 mm steps. In both cases the result is  $v_d = 50.2 (\pm 0.6) \mu\text{m}/\text{ns}$ ; however for mixture A the high voltage had to be at 2.30 kV to guarantee constant drift velocity. Figure 2 depicts the HV plateau curves for one tube. One notices that full efficiency is reached at a value approximately 100 V lower than needed for constant drift velocity across the tube radius. The individual tubes cause a spread in the onset of the plateau by another 50 V. The measurement was carried

out at a rate of approximately 600 counts/s·cm and the efficiency versus radial distance was found to be 100% as close as 0.25 mm to the inner tube-wall.

Figure 3 shows a typical event. The raw TDC data are depicted on the left side, whereas the right part contains corrections for the TDC slope and offset, as well as for the relative alignment of the drift tubes. The solid line gives the reconstructed track  $y = ax + b$  with  $\sigma_a = 0.26$  mrad and  $\sigma_b = 50$   $\mu\text{m}$  with a  $\chi^2/\text{D.F.} = 0.76$ . The reconstruction succeeded in the second attempt only, since points further away from the track than  $5 \sigma_{\text{tube}}$  ( $\sigma_{\text{tube}} = 135$   $\mu\text{m}$ ) were rejected, to exclude  $\delta$ -rays.

Figure 4 depicts the drift-time distribution sampled over 1000 events. The full y-scale corresponds to the tube radius, i.e. 5 mm or 100 ns. The peak width is caused mainly by the finite size of trig 2 \* trig 3. The contribution of  $\delta$ -rays can be seen on the low y-side of the peaks since the TDCs stop on the first pulse after the common start.

Figure 5 gives the distribution of points participating in the track reconstruction as a function of their distance from the track (expressed in units of  $\sigma_{\text{tube}} = 135$   $\mu\text{m}$ ). The dotted line is calculated assuming a Gaussian distribution.

The non-statistically distributed measurements are 6.6% of the reconstructed track. Their main source is  $\delta$ -rays, but electronic cross-talk, bad fiducials, and non-uniform drift velocity are additional sources. It is important to exclude these coordinates, since especially in the case of  $\delta$ -rays their effect does not average out.

Finally the  $1/\sqrt{N}$  law was checked for the spatial resolution over the range  $5 \leq N \leq 21$ . There is good agreement with the data for  $\sigma = (156 \pm 5)$   $\mu\text{m}/\sqrt{N}$ , as shown in Fig. 6. The somewhat higher value for  $N = 1$  as compared with  $\sigma_{\text{tube}} = 135$   $\mu\text{m}$  arises from the rejection of points farther away than  $5 \sigma_{\text{tube}}$ , without taking into account the change of  $N$ .

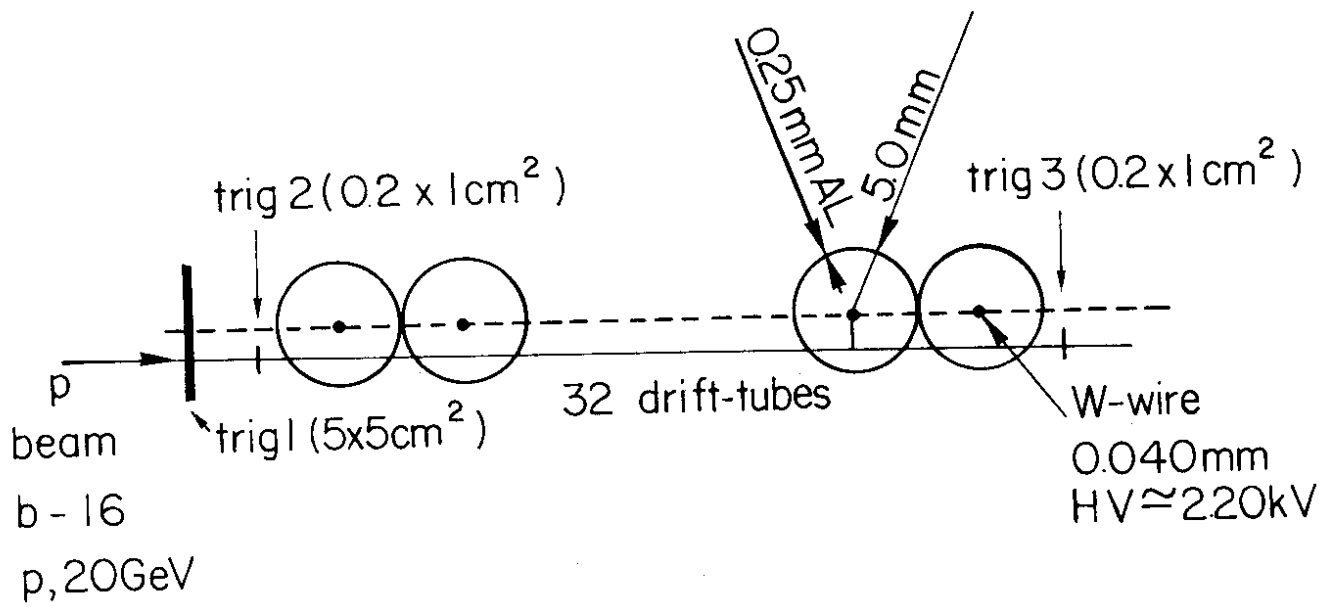
We thank Dr. Kouptsidis and Messrs. P. Bergus, R. Harfield, G. Muratori, D. Osborne and P. Reddick for technical help and support.

REFERENCES

- 1) ECFA-LEP Working Group, see, *in* 1979 Progress Report (ed. A. Zichichi), SSG11 (p. 179), SSG13 (p. 197), SSG14 (p. 217).
- 2) ISABELLE Research Project, U. Berger et al., BNL-T20 (1978).
- 3) D. Barber et al., Phys. Reports, to be published; and MIT-LNS preprint No. 107, First Year of Mark J.

Figure captions

- Fig. 1 : Experimental set-up.
- Fig. 2 : Efficiency versus high voltage. Solid line: gas mixture A. Dotted line: gas mixture B.
- Fig. 3 : Display of a typical event with two rejects according to  $y \geq 5 \sigma_{\text{tube}}$ .
- Fig. 4 : Integrated drift-time distributions for the complete drift-tube array.
- Fig. 5 : Frequency of  $(y_{\text{meas}} - y_{\text{reconstructed}})/\sigma_{\text{tube}}$  for a reconstructed track. Solid line: measured values. Dotted line: statistically calculated values assuming a Gaussian distribution.
- Fig. 6 : Spatial error as a function of measured points.



Electronics:

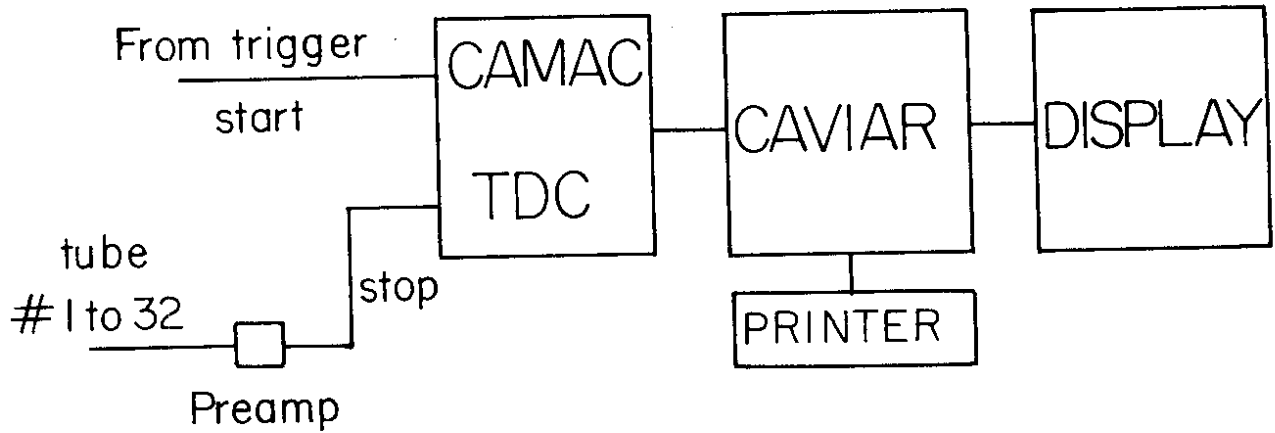


Fig. 1

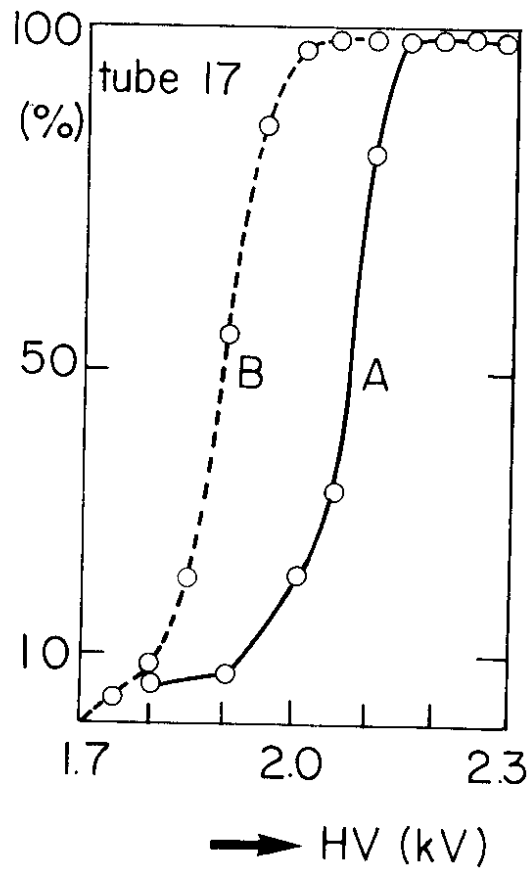


Fig. 2

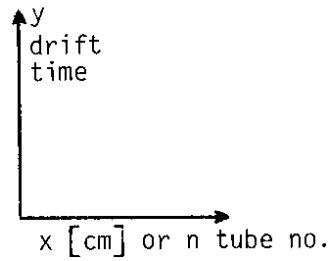
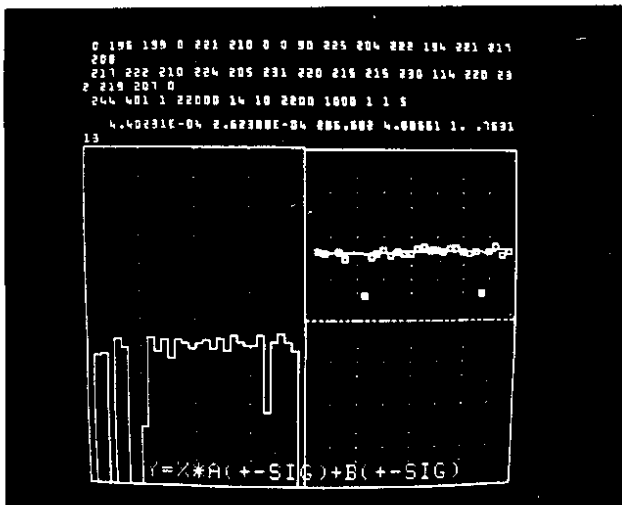


Fig. 3

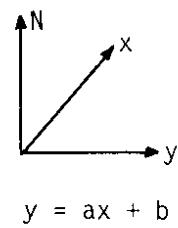
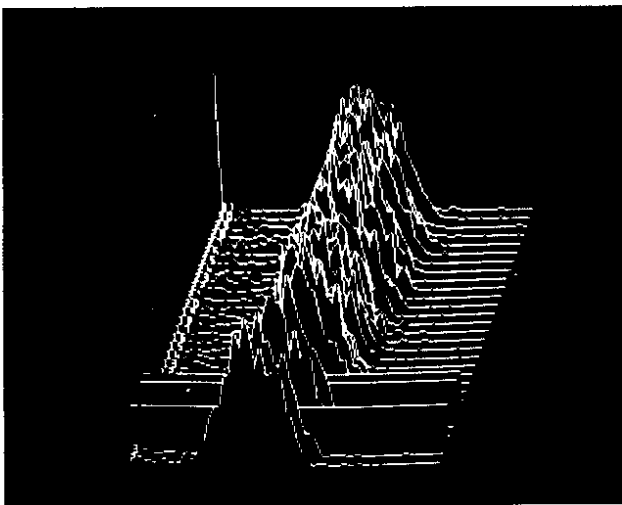


Fig. 4



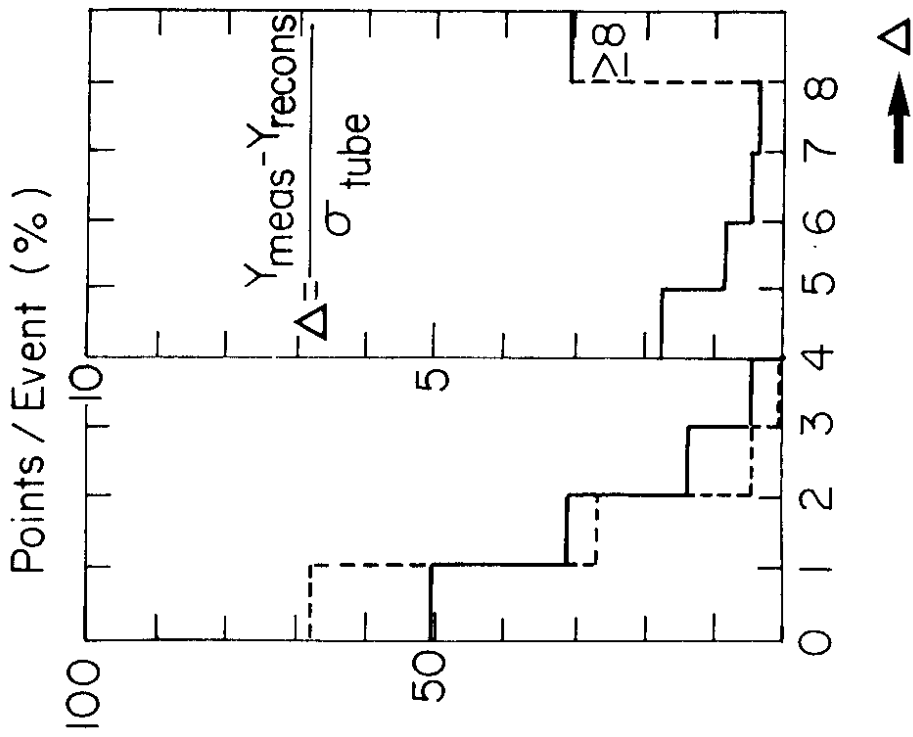


Fig. 5

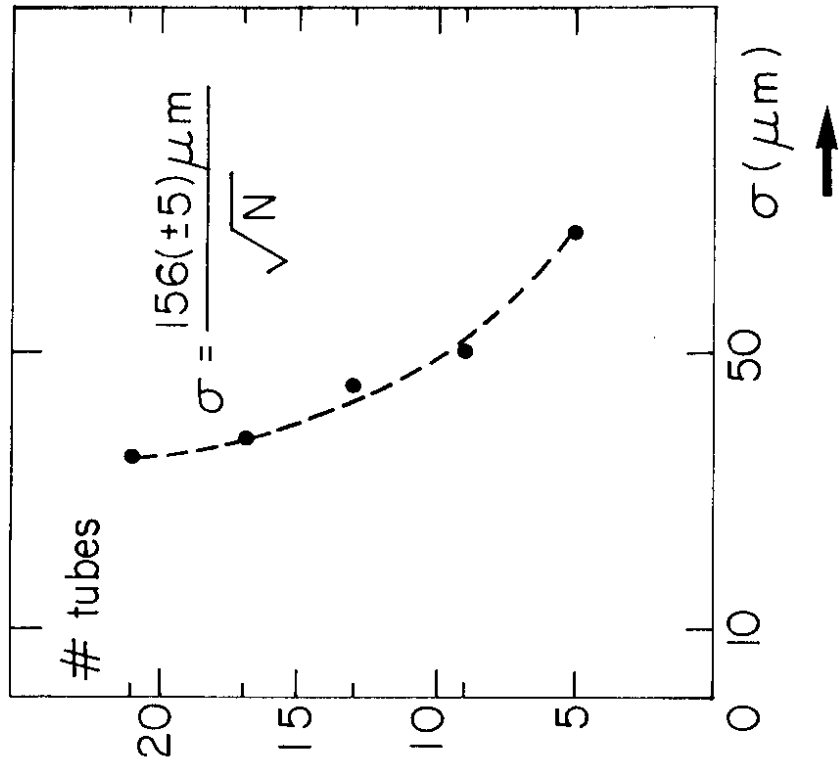


Fig. 6